Penerbit Akademia Baru

Progress in Fluid Power, Mechanisations and Mechatronics

Journal homepage: www.akademiabaru.com/promecha.html
ISSN: 2672-7218

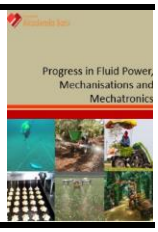

MHeLFAGV: A Remotely Controlled Mini Fork-loader for Confined Area Operation

Open Access

Addie Irawan[1,*], Akhtar Razul Razali[2], Sheikh Norhasmadi Sheikh Ali[3]

[1] Robotics & Unmanned Systems (RUS) research group, Faculty of Electrical & Electronics Engineering, Universiti Malaysia Pahang, 26600 Pekan, Pahang, Malaysia
[2] Manufacturing Focus Group (MFG), Faculty of Mechanical Engineering, Universiti Malaysia Pahang, Malaysia
[3] Vacuumschmelze (M) Sdn. Bhd, Lot 3465, Tanah Putih, 26600 Pekan, Pahang, Malaysia

ARTICLE INFO

Article history:
Received 5 July 2018
Received in revised form 4 August 2018
Accepted 2 September 2018
Available online 17 September 2018

ABSTRACT

This article presents the first phase of development of a mini fork-loader system for heavy payload application in a confined area, named Mini Heavy Loaded Forklift Autonomous Guided Vehicle (MHeLFAGV). With emerging of new technology such as Automated Guided Vehicle (AGV) and Remotely Controlled Vehicle (RCV), the forklift operation able to be done with unmanned and assistance through remotely controlled for both long and short distances. However, most of the AGVs/RCVs in the market are available for the certain standard size of the area of work which is sometimes unable to meet the user requirement especially for the confine and narrow area deployment. Therefore, this project has initiated to solve the industrial need by designing and developing MHeLFAGV with RCV concept with swallow mechanism to handling between 20-200kg of the copper spool at the confine warehouse. MHeLFAGV is designed to suit with the 170cm x 270cm square area that configured with tri-tips and 2-axis of fork-lifter to pick-and-place and extend-retract a spool item operation respectively. The omnidirectional mechanism was chosen by configuring four industrial-scale mecanum wheels as MHeLFAGV's wheels. Moreover, this customized fork-loader unit also equipped with absorber unit to deal with any uneven terrain that essential for mecanum wheel and its movement topology. Wireless remote controls and mainly with two stages of controller boards; Board 1 and Board 2 was developed as a controller and monitoring unit of the system. The intensive tests and experiments were done by operating both indoor and outdoor operation on MHeLFAGV. The structure model was verified with finite element analyses and the motion algorithms the were validated in the wide terrain area with Global Positioning System (GPS) as its waypoint tracer.

Keywords:
Mini fork-loader, swallow-based mechanism, omnidirectional, heavy payload

1. Introduction

Autonomous and semi-autonomous vehicles are becoming one of the mobile robotic systems that commonly used as a surveyor, military and assistant unit. In assisting point of view, this system

* *Corresponding author.*
E-mail address: addieirawan@ump.edu.my (Addie Irawan)

also commonly used in manufacturing area such as factories and warehouses that required systematic fast and minimum number of labor especially for a task that involved dangerous or hazardous area. This system named as an automatic guided vehicle (AGV) which is commonly developed and commercialized by some companies including such as Toyota, Hitachi, Savant Automation, JBT Corporation and many more. Most of the AGV in the market were developed for heavy-duty tasks (more than 100kg of payload) and required a sufficient space (big size) whereby the area is commonly well prepared for AGVs deployment. It is different for the cases that AGVs which are installed on a new landscape that is not ready for a driven machine such as for confine and narrow warehouse area. Moreover, some of the confined area in warehouses keeping heavy products and inventories which is very difficult to handle by humans manually. Therefore, this paper has taken the initiative to develop a new mechanism of AGV for heavy payload at the confine and narrow area with improved autonomous elements.

There are several issues have been tackled to increase the efficiency of AGV including its autonomy such as steering [1-4] and flow control [5-7], pick-and-place tasks, localization/mapping [8,9] and energy efficiency [10]. These issues are according to the application that needs some improvement in inventory handling and management. For the case of a confined area and massive inventory handling, the mechanism on the pick-and-place process is very crucial since small size and stable AGV design is needed. Several control approaches were deployed in the pick-and-place process by using intelligent control, adaptive control, vision/image processing, and event hybrid visual servoing techniques as reported in [11,12]. In term of picking and placing operation that mostly used grasper unit or forklift system also another part the issue that needs to be emphasized in developing AGV.

A vehicle with forklift unit mainly consists of two main parts which are a fork-loader unit system (also known as gripper and elevator) and a drive system. A fork-loader design built with minimum two pointing outward acting as fingers to elevate and hold any targeted load. Generally, two axes of motion are used for a fork-loader for a pick-and-place task. Most of the current fork-lifter and heavy machine technology especially that required time consuming (fast and efficient) in mass production, had evolved to be more automated such as Remotely Controlled Vehicle (RCV) and Automated Controlled Vehicle (AGV). This technology major controlled by particular electronics system that able to minimize labor cost, time-consuming and increase the efficiencies in a long hour workflow.

Therefore, this research and development have taken the initiative to involve on design and develop flexible heavy loaded vehicle named Mini Heavy Loaded Forklift Autonomous Guided Vehicle (MHeLFAGV) (patent applied) [13] specifically for maneuvering in a confined area.

2. Vehicle Mechanism, Maneuverability and Wheel Selection

In order to improve maneuverability and practical applications of the wheel mobile robot in the last years, a variety of mecanum wheel have developed. As shown in Figure 1 the mecanum wheel is a family member of Omni-wheel that consists of rollers around the surface body of the wheel depending on the size of mecanum. The mechanism's roller assembled in ‘axis-b’ is slight skew to ‘axis-a’ wheel which usually 45° degrees of angle between ‘a’ and ‘b’ axis. Moreover, along with the peripheral of the big core wheel, mecanum wheel contained with the sub-wheels that have the axis perpendicular to the axis of the core wheel. The core wheel able to rotate around its axis as any standard wheel since the smalls wheels rotate in the direction of the core wheels’ axis, the core wheel itself can then move on own axis. Concerning the Omni-wheel configuration in Figure 1 it shows that omnidirectional mobile robot or vehicle with Omni-wheel work and maneuvered by a specific wheel with so many wheels integrated [14,15]. In the development of Wheel Mobile Robot (WMR), various

configuration of design that considers the mobility and maneuverability of the robot by considering the effectiveness of the tire architectures and Figure 2 show the classification of tires that commonly used in WMR system.

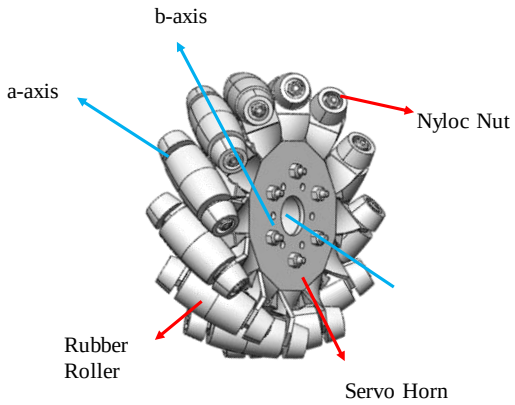

Fig. 1. Mecanum wheel design for the mobile robot system

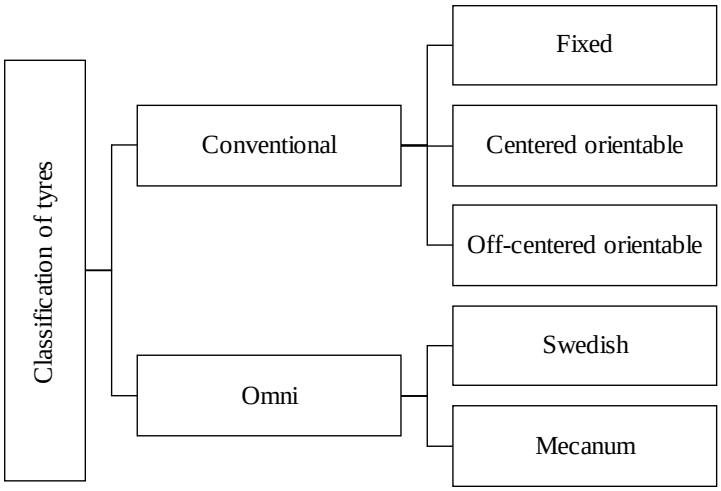

Fig. 2. Classification of tires for wheel mobile robot

According to the Astrom *et al.*, [16] mecanum tire movement required independent wheel control either in speed, torque and rotation to realizing its omnidirectional movement capability as shown in Figure 3 [16]. Figure 3 shows the rotational of selecting omnidirectional mechanism with skid-steering and 4-wheeled drive mechanism compared to the 4-wheeled mechanism with rear drive and rack steering. The omnidirectional vehicle will not be intense to turn its body at cornering route as shown in Figure 3(a) compared to the 4-steered vehicle with rear drive and rack steering as shown in Figure 3(b). This situation is practical if the square size of omnidirectional is sufficient enough with the passing route and peer walls.

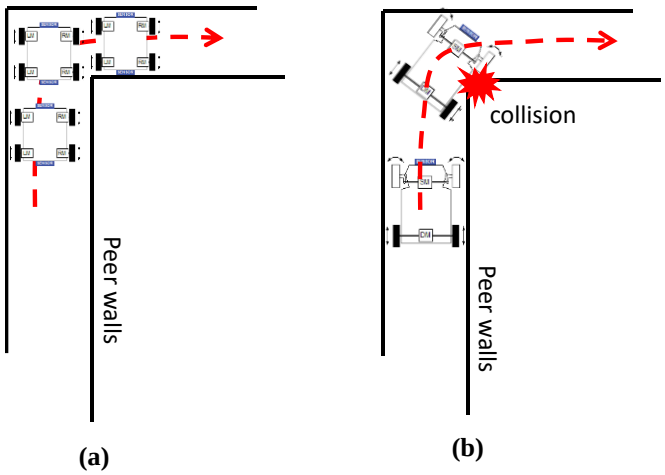

Fig. 3. Example of rotational used of skid-steering 4-wheeled drive vehicle mechanism for the confined area: (a) situation of cornering by the rear 4-wheeled drive and skid-steering vehicle, (b) situation of cornering by the rear drive and rack steering vehicle

As depicted in Figure 3, a 4-wheeled vehicle with mecanum wheels has the different topology of movement compared to steering type 4-wheeled vehicle. For example, as shown in Figure 4(b), if running mecanum wheels on one diagonal in the opposite direction to those on the other diagonal it will cause sideways movement. It is a different situation in Figure 4(e) where the mecanum wheels rolling on one side in the opposite direction to those on the other side will causing the vehicle to spin on its center of the body (CoB). Therefore, combinations of these basic motions as shown in Figure 4, allows the 4-wheeled vehicle to perform omnidirectional movements with skid-steering.

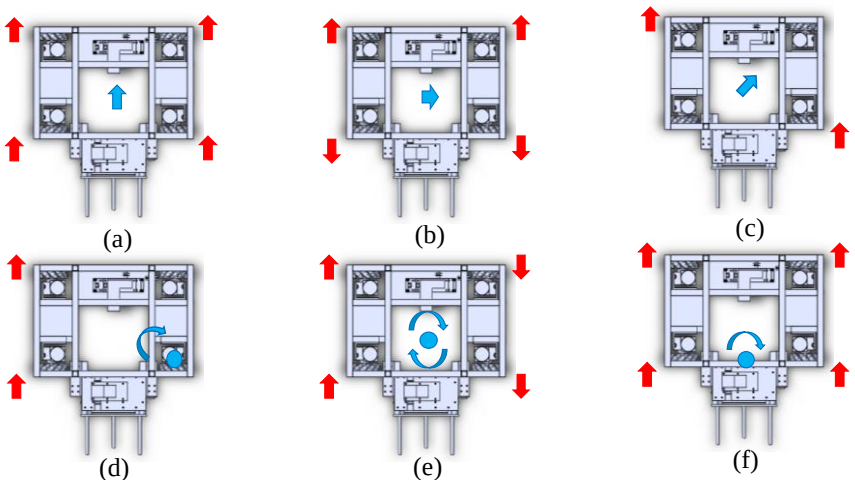

Fig. 4. Basic movement of the 4-wheeled vehicle with mecanum wheels (a) straight ahead, (b) sideways, (c) diagonal, (d) turn around, (e) concerning/spinning, (f) turn of the rear axis

3. Frame Structure and Grasper Mechanism

The main part that needs to be considered in MHeLFAGV structure design is the chassis part. The chassis should be able to withstand a load of maximum 200 kg as well as mechanical components

such as ball screw and linear guide. Moreover, the chassis design also needs to consider electrical and electronic components such as controller unit and sensors. Figure 5 shows the MHeLFAGV design that considers all the mentioned elements as well as inventory store sizes where the copper spools are placed.

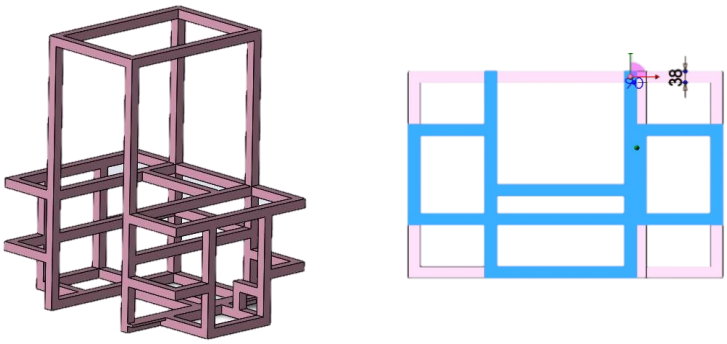

(a) **(b)**

Fig. 5. MHeLFAGV Chasis Design: (a) isometric view, (b) top view

As shown in Figure 5(b), the C-shaped design was referred which allows some spaces inside the body of the chassis for aiding in the spool transferring. The highlighted blue color in Figure 5(b) shows the base of the chassis in the form of C–shaped. MHeLFAGV's chassis was made of a 3 millimeter thick hollow rectangular metal (986×700) millimeter at the bottom, supported by parallel and correctly welded profiles at the top in order to be able to stand the heavy weight of the other components and the maximum expected load. Also, the base is surrounded by the same perpendicular profile to hold the covers and withstand the unexpected load, collisions, anything unpredicted or further from the project subject and other applications. In order to ensure mecanum wheel always touching with the floor and adapting uneven terrain, a suspension is designed for MHeLFAGV. This design is crucial to ensure the basic motion as shown in Figure 4 can be realized. As shown in Figure 6 an absorber unit was installed and configured which flange is used at the bottom of mounting to wheel holder and rod for mounting with the chassis.

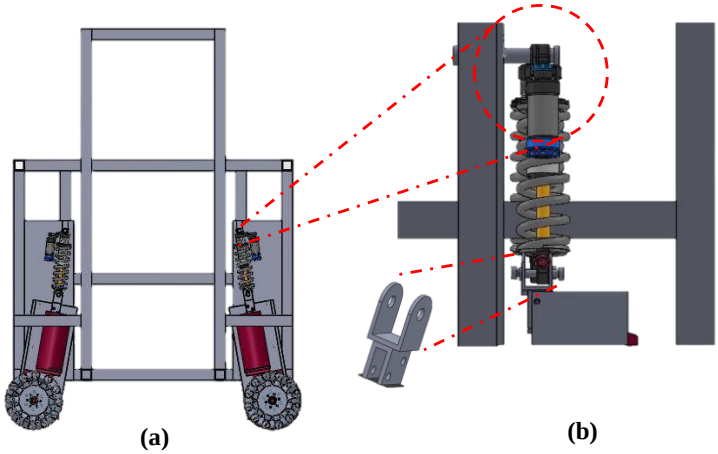

(a) **(b)**

Fig. 6. Absorbe r and Suspension system design for MHeLFAGV Chasis Design: (a) MHeLFAGV frame view, (b) zooming view on absorber mounting

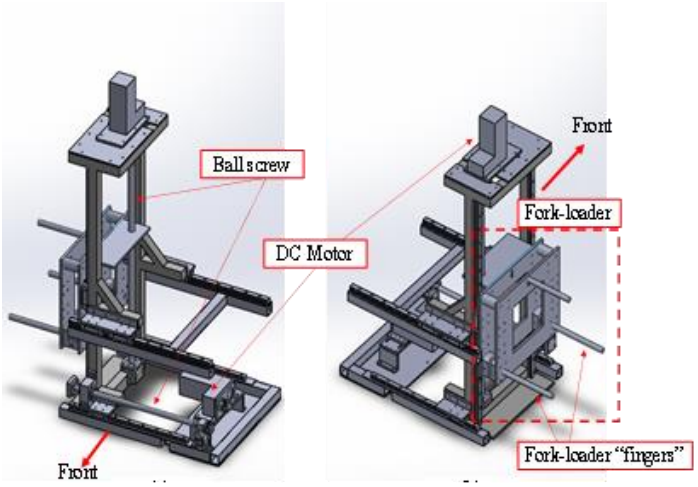

(a) (b)

Fig. 7. MHeLFAGV Forkloader Platform: (a) rear side view, (b) front side view

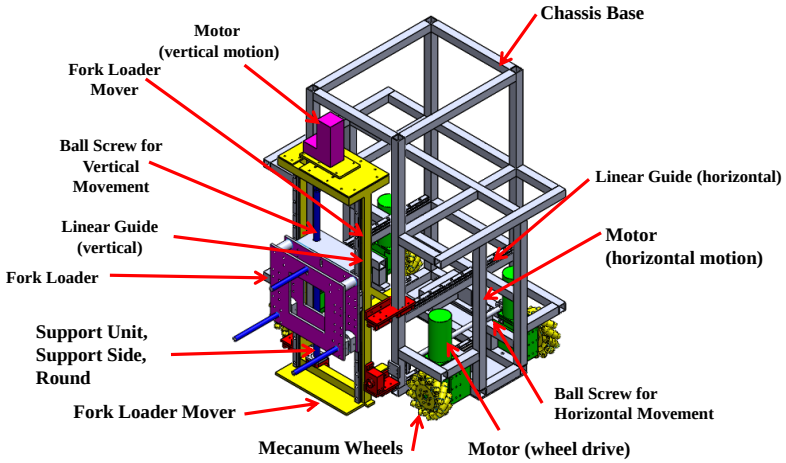

Fig. 8. MHeLFAGV system structure model overview

For the case of grasper unit fork-loader is designed with (225×400×1000) millimeter size, held by 4 L-squared aluminum plates welded to the side for suspending the platform to an adequate position as shown in Figure 7. This platform material also made from hollow rectangular metal same as used for chassis design. Also, this platform will be the crucial part in moving the fork loader in and out to pick the spool. Thus, the welded parts need to be very precise in a 90-degree angle to maintain a good movement. An overview of the MHeLFAGV system mechanical structure is shown as Figure 8.

4. MHeLFAGV Control System and Basic Operation

4.1. Omnidirectional Movement Control with Mecanum Wheel

This development of MHeLFAGV is emphasized on remote control mode and with auto-detection on targeted load as autonomous elements. Remotely control is essential at this level as it is the first thing that needs to be provided to meet the client need. As MHeLFAGV is a mecanum wheeled vehicle, the movement of this AGV system is programmed and design following the basic motion of mecanum movement as discussed in Section II and shown in Figure 4. Generally, the whole project consists of three phases of development. In the first phase of development wireless remote control system was established with wireless radio frequency (RF). The overall connection of MHeLFAGV

control unit can be illustrated as Figure 9 where two mainboards; Board 1 for all motion control on MHeLFAGV drive system including Forklift unit and Board 2 for data acquisition or monitoring to Mini personal computer (PC).

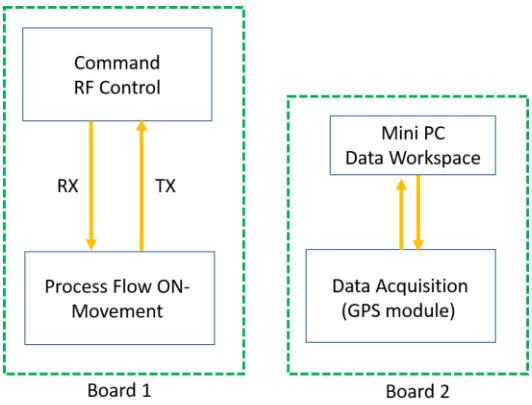

Fig. 9. Overall control system interconnection in the MHeLFAGV controller unit

As for the Board 1, the system consists of motion and drive control which Arduino Mega 2560 as core processor and industrial scale XDC2460 Roboteq as Dual-driver for DC motor attached on each mecanum wheel and forklift axes. Figure 10 shows the flow of connection for Board 1 that emphasized on remotely control using RF connection as well as displaying tuning speed for a mecanum wheel from the potentiometer and receiving a feedback signal from the ultrasonic sensor. In detail overall of MHeLFAGV Board 1 consist of modules of three DC motor controller connected to microcontroller pulse width modulation (PWM) pins as shown in Figure 11. The potentiometer is connected to an analog pin of the microcontroller in which function to set up and calibrate the PWM input to DC motor controller in the range of 0-255 bit monitored via Liquid Crystal Display (LCD) that connected to the microcontroller. As shown in Figure 11 there is a total of 6 DC motors used in the MHeLFAGV system and four of them is for mecanum wheel and the other two is for Forklift unit.

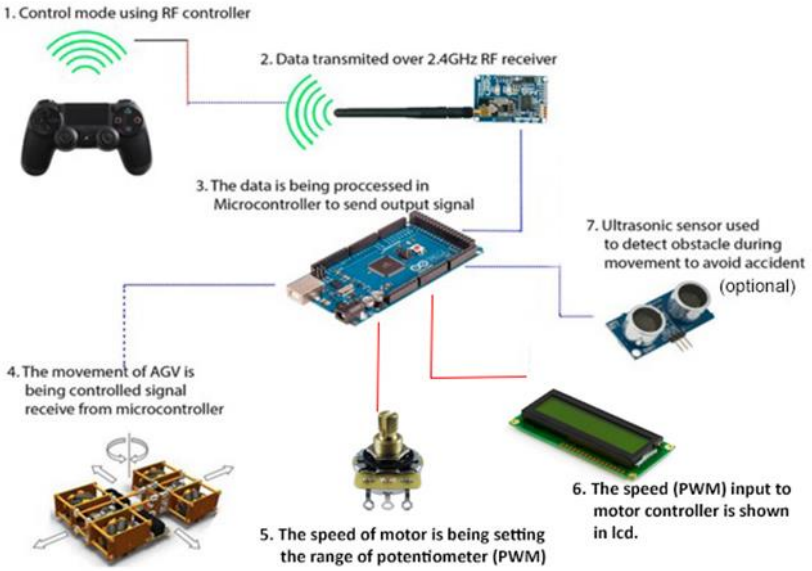

Fig. 10. The general internal connection of Remotely Controlled System (Board 1)

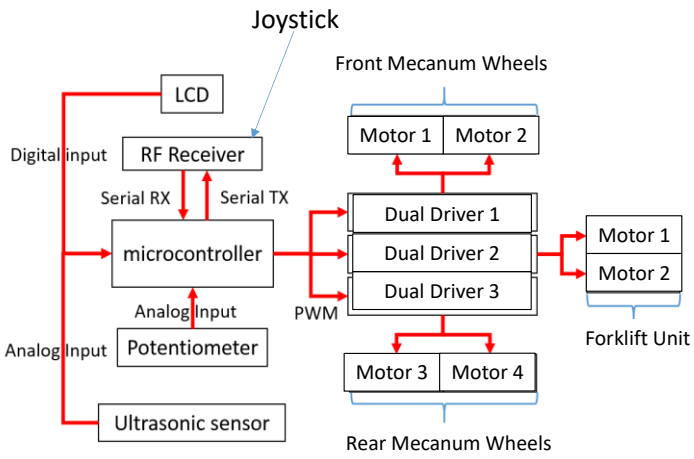

Fig. 11. The Board 1 internal modules and its connection with targeted devices

Moreover, each couple of DC motor on mecanum wheels are drive with Dual motor driver (XDC2460) and this controller able to drive both counter-clockwise (CCW) and clockwise (CW) since the driver is a full-bridge circuit. Figure 12 shows a bit zoom-in for a dual driver control on each couple of DC motor in MHeLFAGV from Board 1 and Joystick as a remote controller.

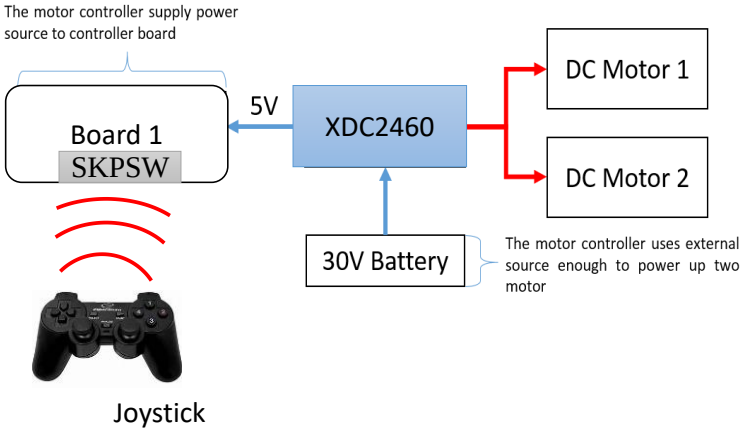

Fig. 12. The detail dual driver XDC2460 controlling couple DC motor from Board 1

In order to operate and programmed XDC2460, simple rule of the range was followed as shown in Figure 13. The overall value of PWM signal range is between 0-255 with the range between 0-127 is for CW direction, and 128-255 is for CCW direction at a certain speed. To stop the motor, the value of PWM must be at 127, and this dual driver has an internal configuration that can be configured using utility manufacturer software as shown in Figure 14. The configuration includes the acceleration, deceleration, power input, power output, etc. In order to stop the motor smoothly, this dual driver was configured in the range of stop deadband. By increasing the deadband to stop the PWM value closer to 127 will stop the motor smoothly.

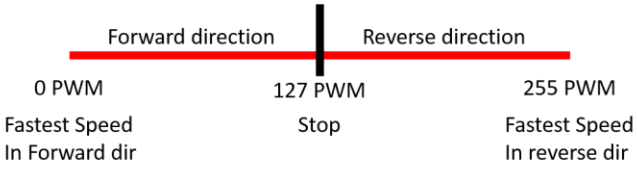

Fig. 13. The enable input range of XDC2460 (PWM input range)

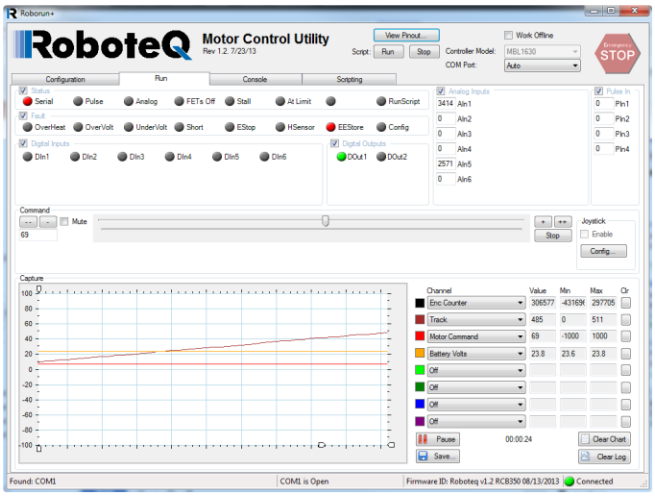

Fig. 14. The manufacturer utility software of dual driver setting

Fig. 15. Key-Binding control of Joystick used for MHeLFAGV remote controller

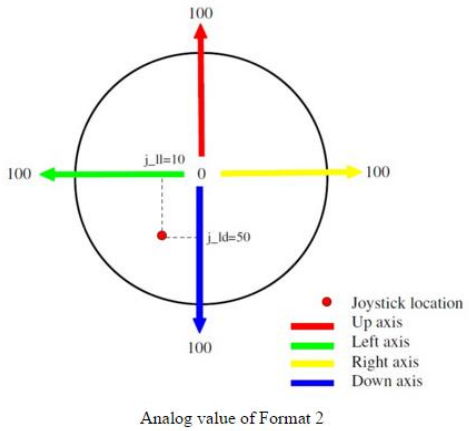

Fig. 16. The joystick control mapping reference

For the remote control unit, as shown in Figure 15, each button is programmed with a particular function of movement direction. Moreover, the joystick has the same function as potentiometer where it is producing range number such as PWM instead of the analog voltage. The joystick can be slowly toggled to control MHeLFAGV's speed. The joystick system produces a range of value output between 0-100 each axis of the joystick like '*X*' and '*Y*' axis as shown in Figure 16. Therefore, to realizing the joystick function, a function is programmed with the flow as shown in Figure 17. The four variables are up, down, left, and right was defined. When the user moves the joystick in any direction, the value of these four variables range from 0 to 100 as shown in Figure 18 are generated. Left and right button on the joystick will have four independent variables. Therefore, the movement topology concerning the Figure 4 in Section II, the code module has been prepared is organized and shown in Figure 18.

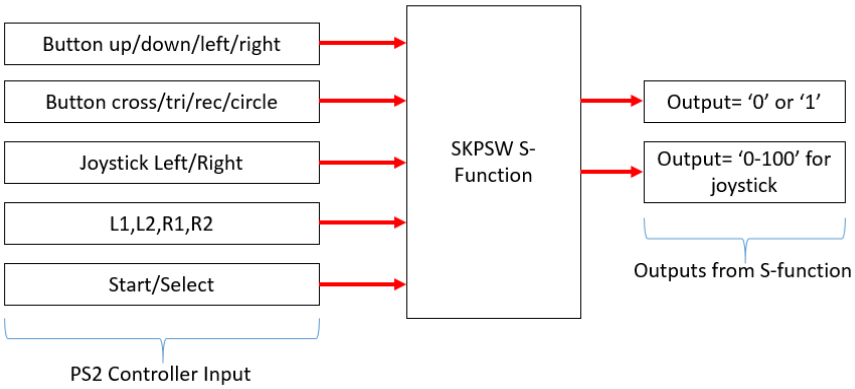

Fig. 17. Block Diagram of SKPSW function code module in the microcontroller

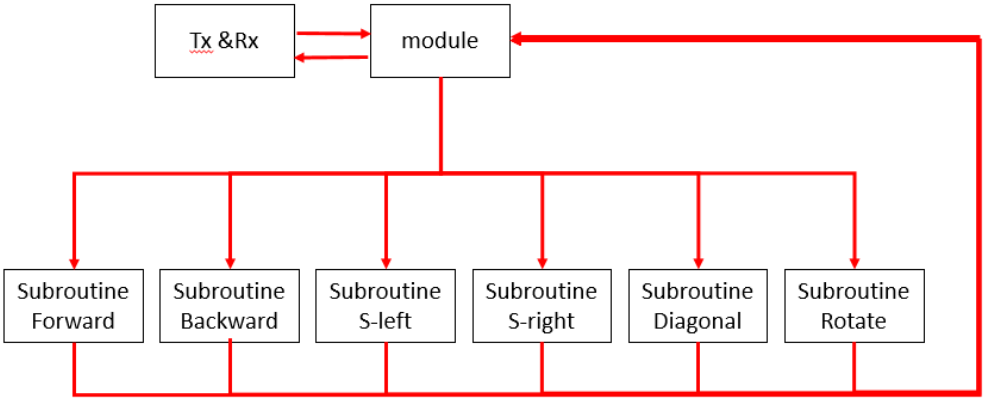

Fig. 18. Overall subroutine code module for MHeLFAGV basic movement

The development is of Board 2 a bit simple in this phase where a GPS system was installed and programmed for MHeLFAGV waypoint monitoring. Installed GPS is programmed to give information of vehicle coordination and save in the portable mini PC. The function code of GPS is developed to acquire the encoded data from the GPS module; the value of longitude and latitude of the MHeLFAGV coordination. Figure 19 shows a diagram of the function code module that programmed in Board 2.

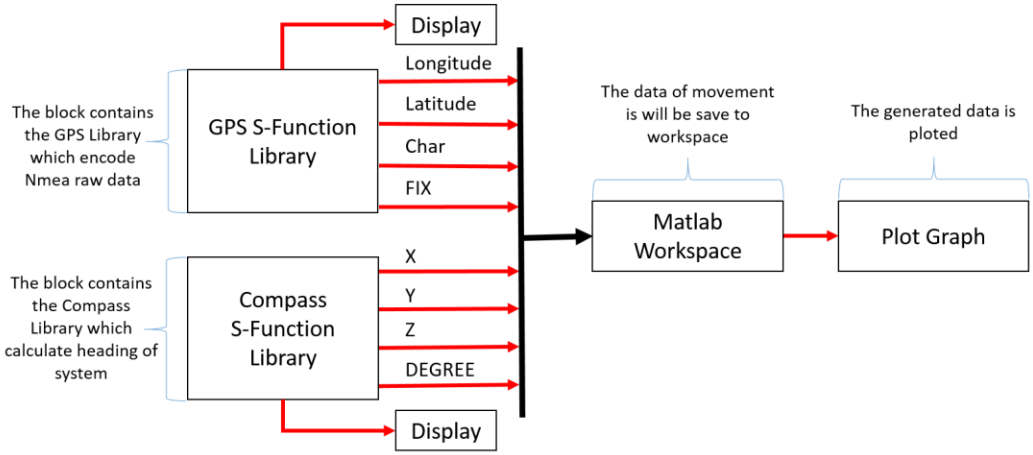

Fig. 19. The GPS system embedded code in Board 2

4.2. Forklift Precision Control and Locking System

On the Forkloader unit system, the grasping-and-swallowed mechanism is applied [17], in which the load is kept inside the main body while the fork-loader is traveling or transferring its load. This mechanism is designed to ensure the full item is appropriately grasped and placed inside the MHeLFAGV's body to retain the center of gravity (CoG) of the vehicle during movement and to ensure the safety of inventory logging (quality assurance). A 2-axis Forkloader system is designed for the MHeLFAGV system, as shown in Figure 7. The motion of the two axes allows loading and unloading of the picked material; the *Y*-axis is used to elevate or lift the fork-loader, while the *X*-axis is used to move the fork-loader inside and out of the MHeLFAGV's body, as shown in Figure 20. Board 1 is the controller unit for Forkloader in which dual driver 2 is configured to drive both *X*-axis and *Y*-axis of the Forklifter as notified in Figure 20. This movement is different from that found in the common forklift system, in which the four wheels need to move forward or backward to get closer to the load (non-holonomic mechanism). On the other hand, as shown in Figure 20, the ball-screw rotation is used in MHeLFAGV's Forkloader unit since the targeted payload is between 50kg and 200kg. Concerning Figure 7, the motion and movement of the fork-loader are driven by a ball screw that is connected to the shaft of the DC motor.

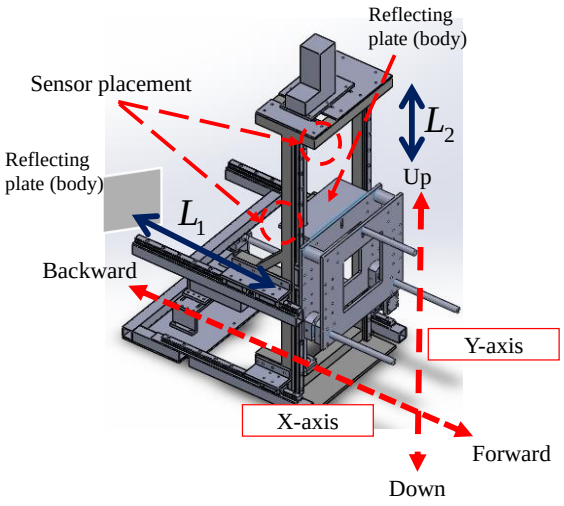

Fig. 20. Grasping-and-Swallowed mechanism and sensor configuration

Table 1
The main components configured in the Forklifter control system of MHeLFAGV

Component	Brand	No. of unit	Remarks
High current DC Motor	53mm	2	Geared Motor, 24V DC
Sensor	35mm	2	1cm resolution, 5V DC
Dual Motor Driver	9mm	1	Dual Channels, 60V DC
Board 1	7	1	5V DC

As shown in Table 1, ultrasonic HC-SR04 with a range from 2 cm to 400 cm (1 cm resolution) is used as a feedback for each axis of the Forkloader motion. This ultrasonic sensor is attached as shown in Figure 20 and is used to measure the distance between the fork-loader and the reflecting plates. The sensors are placed along both axes, such that the beam of the sensor faces the reflection plate, and the plate is used to reflect the "Ping" sound to the sensor. As shown in Figure 20, L_1 and L_2 are notified as the distance measured by the ultrasonic sensor for *Y*-axis and *X*-axis, respectively.

As mentioned in the previous section, a Takagi-Sugeno-Kang (TSK) type Fuzzy Logic Control (FLC) [18] is used for each MHeLFAGV's Forkloader precision control. This FLC is designed with multiple inputs and single output (MISO) crisp error for the distance of each axis motion by considering two state orders: ΔE and $\Delta \dot{E}$. The error for each axis of Forkloader is expressed as Eq. 1.

$$(E_x(\mathrm{t}), E_y(\mathrm{t})) = \begin{Bmatrix} R_x - F_x \\ R_y - F_y \end{Bmatrix} \tag{1}$$

where F_X and F_Y are the feedback measured data from the distance sensors for the axis motion L_1 and L_2, respectively, as shown in Figure 20. Three steps were taken in developing the FLC, as shown in Figure 21, are fuzzification, fuzzy rules (inference mechanism and rule base) and defuzzification. The continuous fuzzy model proposed by [19] is used via fuzzy *if-then* rules to optimize the input variables. The proposed TSK-FLC system is extended with adaptive elements to cater to the windup phenomenon using Proportional-Integrated (PI) Antiwindup method[20], in which *u(t)* is back calculated. The integration element is expected to eliminate overshoot in Forklift first move, whereby the integral state, $\Delta \dot{E}$ to be recalculated to a new value that produces an output when the system reaches to its saturation limit [21]. As shown as Figure 22, the PI Antiwindup element is added to reproduce new antiwindup *u(t)*, which can be expressed in Eq. 2[20]:

$$U(t) = K_p E(t) + \sum_{t=t-T}^{t} \left(K_i K_p E(t) + \Delta u(\mathrm{t}) \mathrm{K}_T \right) K_{TS} \tag{2}$$

where $\Delta u(t)$ is the updated change of TSK-FLC controller output, $K_{TS} = T^{-1}$ which $T = 1\,ms$ of the processing unit sampling time, K_i is an integral gain, and K_T is a back signal control input gain. Noted that, all this gain tuning is done during the experimental session on an actual system of MHeLFAGV Forkloader unit.

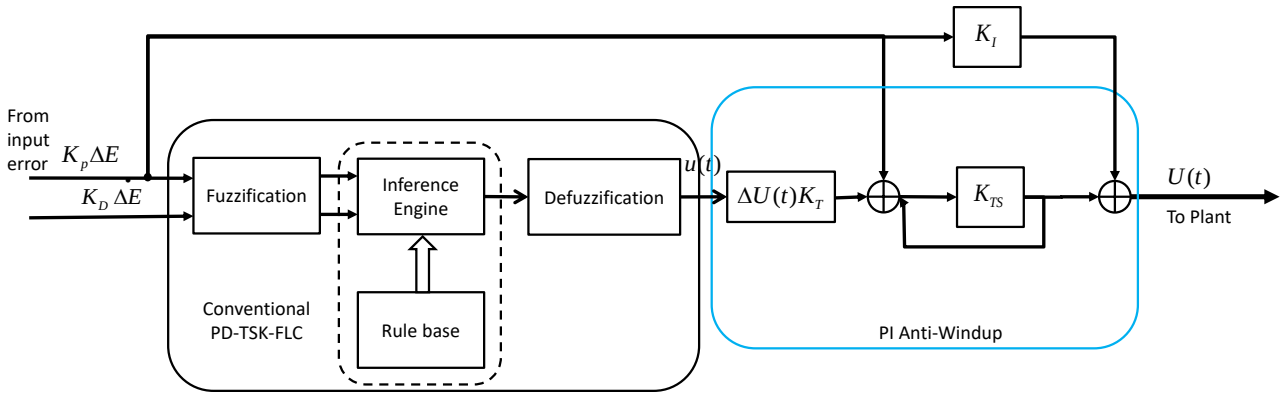

Fig. 22. Block diagram of the proposed PI-Windup-FLC control system for MHeLFAGV Forkloader positioning control

In order to make the load properly tide during the grasping process, a locking is developed with servo motor as a driven device. This servo motor is directly connected to the Board 1 to be controlled by a joystick. Figure 23(a) and Figure 23(b) shows the unlocked and locked modes respectively for this locking system. Once the switch button is pressed on the joystick, the servo shaft will rotate about 90° from its starting point and moves along with it are the two arm linkages. These parts which are connected to the linkages fixed to both shafts rotate about 45° with the shafts along with the parts serve to lock the position of the shaft. Another double pressing needs to be pushed for an unlocked position as shown in Figure 23(b).

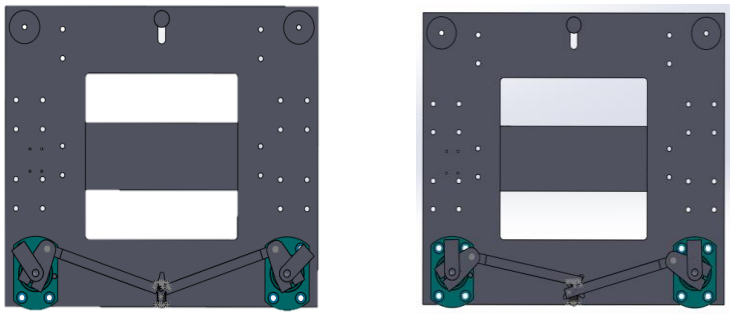

(a) **(b)**

Fig. 23. Additional locking system on fork-loader; (a) Unlock mode, (b) Locked mode

5. Experimental and Results

The designed and developed controller unit has been tested and experiment for validation. The tests and validations are covered; (1) material tests for material and mechanical components selection through finite element analysis (FEA), and motors selections thru static torque and force analysis, (2) omnidirectional movement of MHeLFAGV and (3) forklift precision and locking system performance with the load.

5.1. Finite Element Analysis of Vehicle Structure

Before proceeding to fabrication works a few FEAs were conducted using Autodesk software to analyzing the strength of MHeLFAGV structure withstanding a load of maximum 200 kg as required.

For the MHeLFAGV's main body, two FEA analysis sections were divided which are upper part chassis analysis and lower part chassis analysis. The reason for this analysis division is to ensure body collapse or overturning while carrying the payload. Moreover, each section of the analysis was applied both Von Mises stress analysis and displacement analysis as shown in Figure 24 and Figure 25 respectively. The Von Mises stress is often used in determining whether an isotropic and ductile metal will yield when subjected to a complex loading condition. The lesser Von Mises strain is desired to minimize material distortion as the result of applied load [22]. As shown in Figure 24(a) the lower part of chassis was applied with the load of 1000 N as this frame of the chassis needs to hold the most weight from the fork loader. Therefore, the results show the lower sections maximum value is 0.000126 N/mm^{2,} and the minimum value is 3.8225E-11 N/mm^2. Similar principles were applied to the upper part of the chassis; the lesser Von Mises strain is desired as shown in Figure 24(b). As this part does not need to hold too much weight, the applied load tested is 500N. Thus, the results gave maximum value 12.333 N/ mm^2 and the minimum value is 3.599E-006 N/mm^2 for the upper chassis as shown in Figure 24(b). Concerning both results, the value of the Von Mises strain for these two sections is too small to cause faultiness to the chassis.

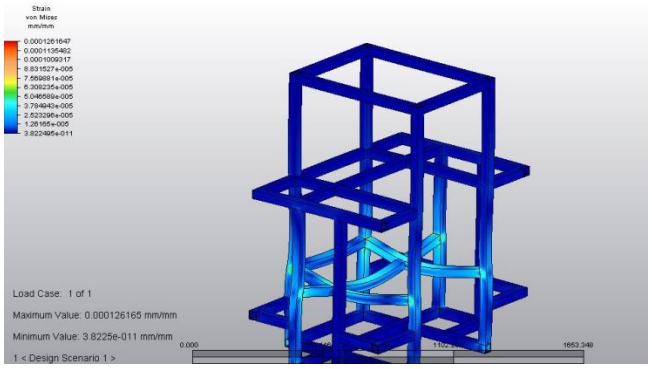

(a)

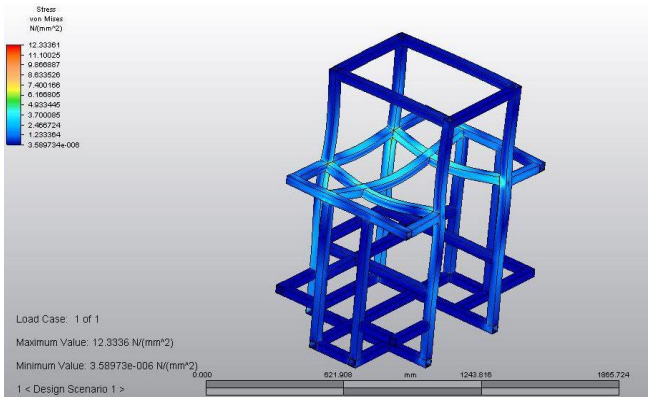

(b)

Fig. 24. Von Mises strain analysis result for the main body chassis: (a) upper body analysis result, (b) lower body analysis result

For the case of verifying withstanding the load applied on the main body chassis, displacement analyses were done. This analysis also divided into lower and upper frame sections as shown in Figure 25 respectively. As mentioned earlier, lower part section where the applied force is 1000 N as this frame need to hold the most weight from the fork loader. As shown in Figure 25(a), lower body was obtained with maximum value of 0.095 mm and minimum value of 0 mm in which shown the chassis is able and safe to withstand load of 1000 N. On the other hand, the upper body chassis analysis

section was done with the half the weight tested than the lower body chassis with an applied load of 500 N. Figure 25(b) shows upper body was obtained maximum value of 0.062 mm and minimum value of 0 mm in which verified that only 0.062 mm displacement that will be taken place if 500 N of force is applied, and this will be given a minimal effect to the MHeLFAGV body chassis.

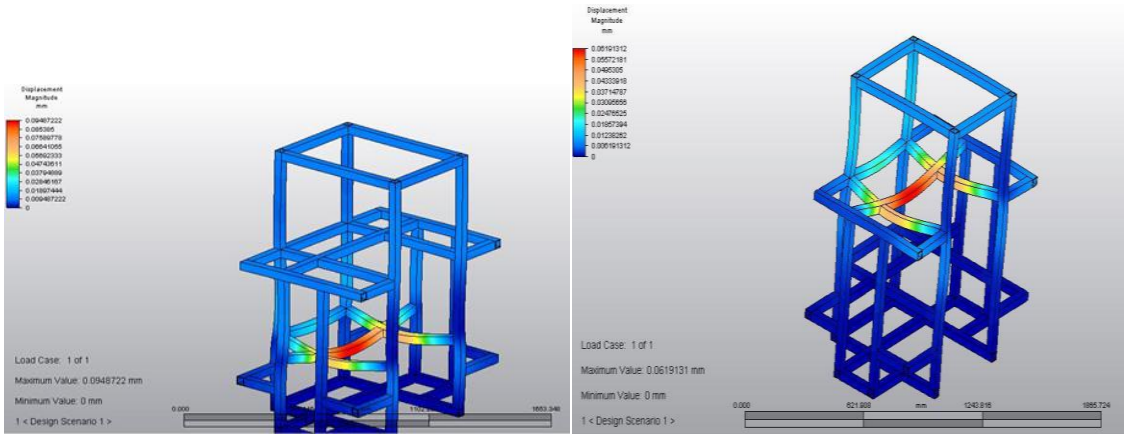

(a) (b)

Fig. 25. Displacement analysis results on main body chassis: (a) upper body analysis result, (b) lower body analysis result

As for the grasper, MHeLFAGV fork-loader structure also has been analyzed before fabrication works done. Similar to the body chassis both Von Mises stress and displacement analysis were done on both track lifter and grasper frame of the MHeLFAGV fork-loader unit. As shown in Figure 26, the maximum value of Von Mises stress for this part is 15.9815 N/mm^{2,} and the minimum value is 0.0206201 N/mm^2 which mean the designed part is too small to cause faultiness to the chassis. On the other hand, FEA result as shown in Figure 27 shows the maximum displacement magnitude is 2.59231 mm and the minimum value is 0 mm, makes the dimension, thickness, and material used for the part design are qualified for the fabrication process.

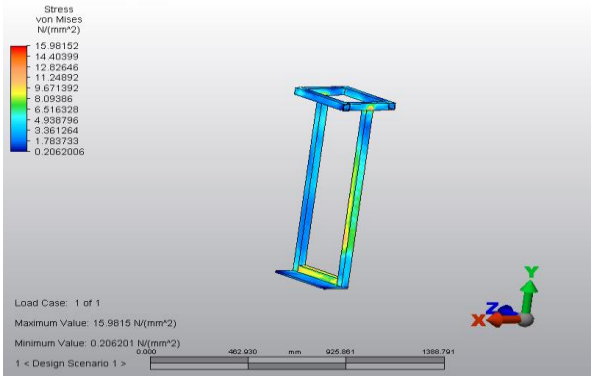

Fig. 26. Von Mises analysis result on track lifter

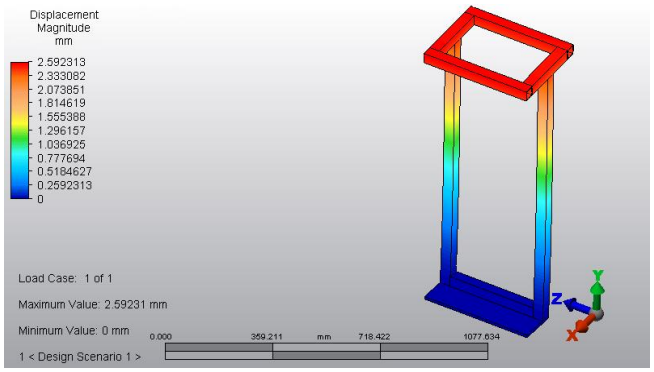

Fig. 27. Displacement analysis result on track lifter

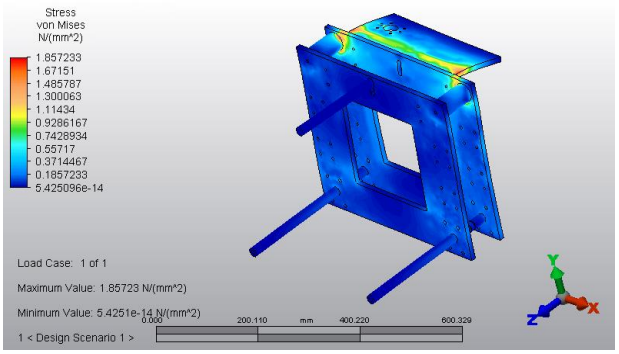

Fig. 28. Von Mises analysis result on grasper

The FEA analysis was further on the grasper part of the fork-loader unit. As shown in Figure 28, 1000 N load was applied in Von Mises analysis of the grasper as this fork-loader unit will be loaded with the maximum weight of 100 kg. As for the results, the maximum value of Von Mises stress for this part is 1.85723 N/mm^{2,} and the minimum value is 5.4251e-14 N/mm^2 as shown in Figure 28. These performances verified that this design grasper frame has a meager chance to cause faultiness. On the other hand, displacement analysis was done on the grasper to ensure the frame can withstand the load applied. As shown in Figure 29, maximum displacement magnitude is 0.0100765 mm, and the minimum value is 0 mm, in which concluded that the dimension, thickness, and material used in the grasper frame design are qualified to be used for fabrication works.

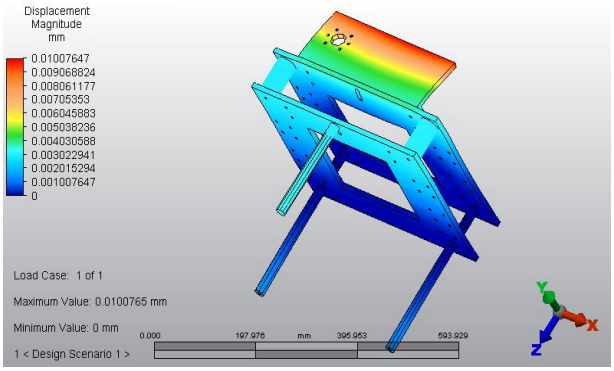

Fig. 29. Displacement analysis result on grasper

5.2. Static Torque and Force Analysis for Motor Selection

In selecting driven devices or motor, a static torque calculation for minimum torque or horsepower determination is done due to the payload and frame structure weight (from materials). For the case of motor selection for mecanum drive, the calculation has been done as follows by considering total tractive effort (TTE) as expressed in Eq. 3 as follows;

$$TTE = R_R + G_R + F_A \tag{3}$$

where R_R is a rolling resistance that calculated from the vehicle weight (*m = 200kg*) and poor concrete ($C_{rr} = 0.02$) for the worse scenario, in which can be calculated as expressed in Eq. 4 as follows;

$$R_R = mC_{rr} \tag{4}$$

That makes $R_R = 4$ kg and grade resistance (G_R) as the force necessary to move a vehicle inclining slope as expressed in Eq. 5 as follows;

$$G_R = m\sin(\theta) \tag{5}$$

Let's targeted climbing slop, $\theta = 10^0$, thus, $G_R = 34.73kg$. On the other hand, F_A can be determined using Eq. 8 as follows;

$$F_A = \frac{mV_{\max}}{a^2 T_s} \tag{6}$$

Let's maximum velocity vehicle, $V_{\max} = 3$ m/s, static acceleration is following the gravitational acceleration and time consuming, $T_s = 6$ s. Thus, $F_A = 10.1937$ kg and this can be concluded that $TTE = 48.9237$ kg @ 489.237 N. For the case of determining minimum torque on motor for each mecanum wheel, TTE value will be used as expressed in Eq. 9 by considering wheel radius, $r_w = 0.0762$ m and resistance factor (R_f) from frictional losses between wheel and axle as well as drag on motor bearing.

$$F_A = \frac{mV_{\max}}{a^2 T_s} \tag{7}$$

Thus, for the case of MHeLFAGV minimum $\tau_w = 42.0573$ Nm by considering max $R_f = 1.15$. The analysis is further with reality checking in order to verify vehicle ability to transmit the required torque from the drive wheel to ground by using maximum tractive torque (M_{tt}) as Eq. 10 as follows;

$$M_{tt} = w_w u r_w \tag{8}$$

where $w_w = 2000$ N and friction coefficient between wheel and ground, $u = 0.8$. Thus $M_{tt} = 119.603$ Nm makes M_{tt} ? τ_w . This can be concluded that the wheel able to provide the traction need in order to propel the vehicle without slipping. Also, concerning the information of the wheel speed, the minimum of the motor's power can be calculated using the Eq. 11 as follows;

$$P_{\min} = \tau_w V_v \tag{9}$$

where the speed of the vehicle in rad/s, $V_v = 39.371$ rad/s. Thus, $P_{\min} = 1.6558$ kW @ 2.2HP. A simple approach is done on calculating static min torque required for forkloader axes driven devices. The maximum load not only consider a copper spool but also the pulling machine weight that makes

minimum total weight for pulling the spool, $w_w = (110kg + 5kg)9.81 = 1150$ N that makes minimum torque required for the motor to drive this axis is $\tau = w_w r_p = 17.25$ Nm with puller radius, $r_p = 0.015$ m. Thus, minimum torque motor to pull the horizontal motion of forklifter must be higher than 17.25 Nm. The same approach is done on calculating motor for lifting or vertical axis of fork-lifter where the motor, spool maximum weight, pulling machine and rail will be considered and total as one maximum weight, $w_w = (110kg + 5kg + 5kg + 20kg)9.81 = 1.4$ kN. Thus, minimum torque required for this axis, $\tau = w_w r_p = 14$ Nm with puller radius, $r_p = 0.01$ m and timing pully will be 36/24 @1.5.

As depicted in Figure 30, the development and design of the MHELFAGV system have a simple shaped platform, with the chassis is welded together to the four pieces of motor plates at the four corners of the chassis where the wheel will be mounted. The MHELFAGV is driven by the four DC motor to the motor plate and fix the wheel nicely. The driving mechanism central part consists of the four brushed DC motor as its prime mover, four mecanum wheels and a chassis which was able to withstand a load of 200kg illustrated in Figure 30. The motor shaft is connected directly to the hub of the mecanum wheel. This design allows for the rollers to be in permanent contact with the locomotion surface, thus allowing a better performance on uneven surfaces. The 3D model of the MHELFAGV is shown in Figure 8 and the pictures of the developed prototype are presented in Figure 30.

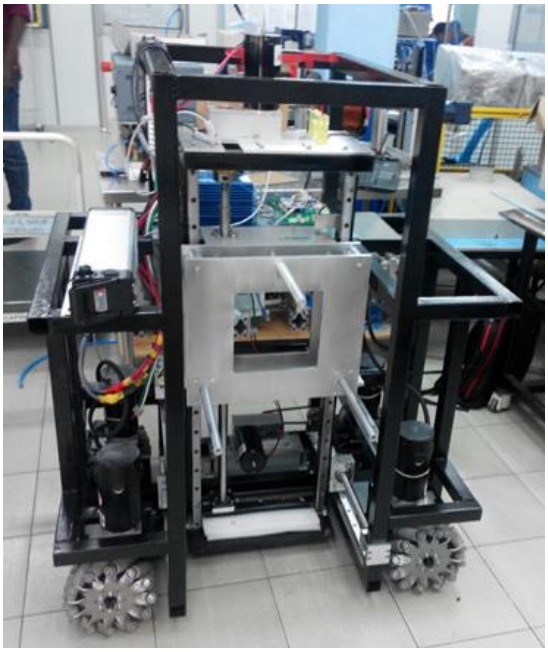

Fig. 30. The Mini Heavy Loaded Forklift Autonomous Guided Vehicle (MHeLFAGV)

5.3. Omnidirectional Movement Tests

The series of field tests have been done on MHeLFAGV to verify a basic movement of mecanum as discussed in Section II, that includes square motion, diagonal motion, zigzagging motion and rounding motion as depicted in Figure 31. Center of the body (CoB) of MHeLFAGV is becoming a reference for its waypoint and also the position of the GPS module. A reference point also has been created as shown in Figure 31(b) as centroid for MHeLFAGV movement.

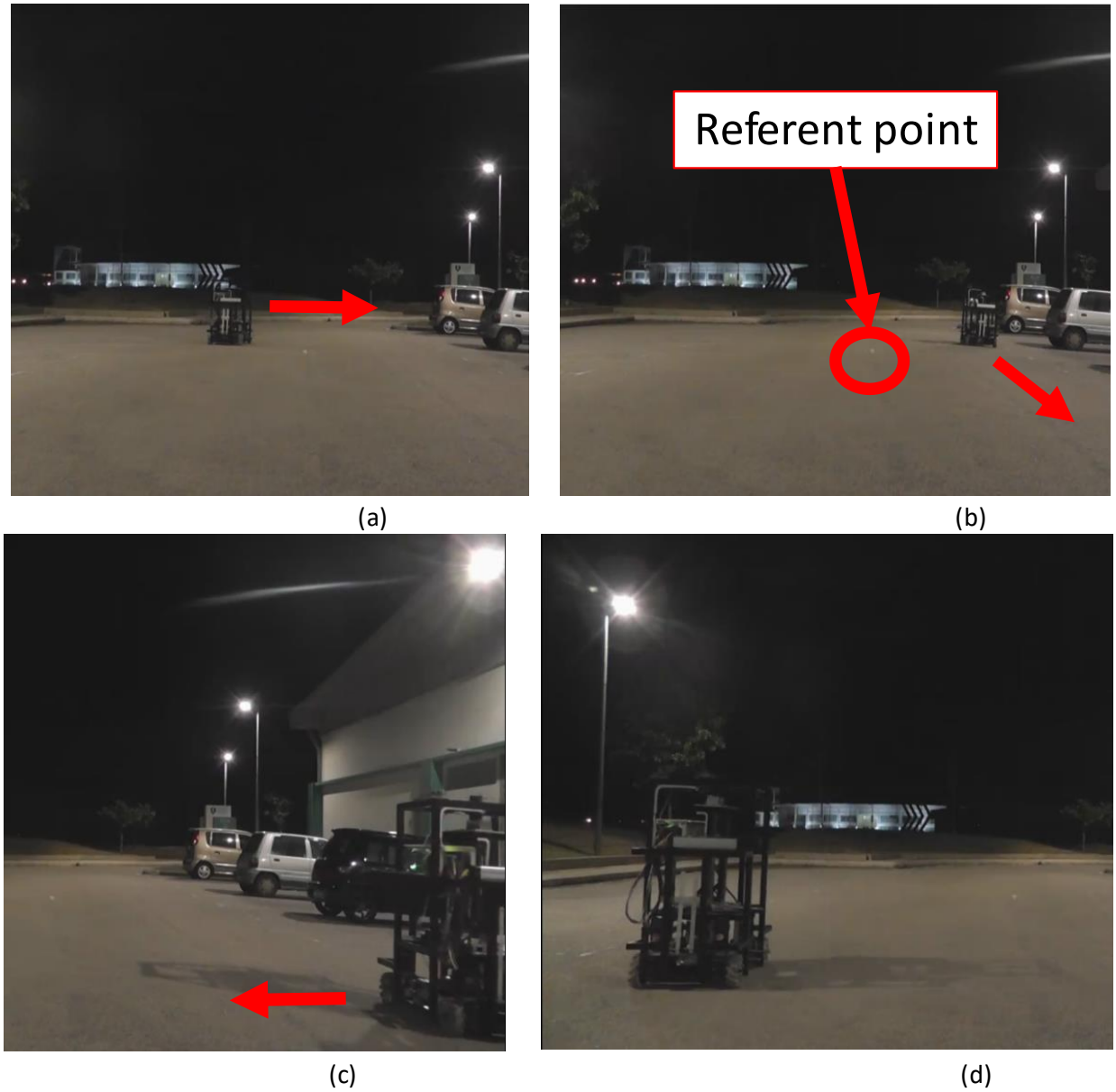

Fig. 31. Snapshot of square motion experiment on MHeLFAGV at almost flat terrain; side left, (b) forward, (c) side left (d) backward movement

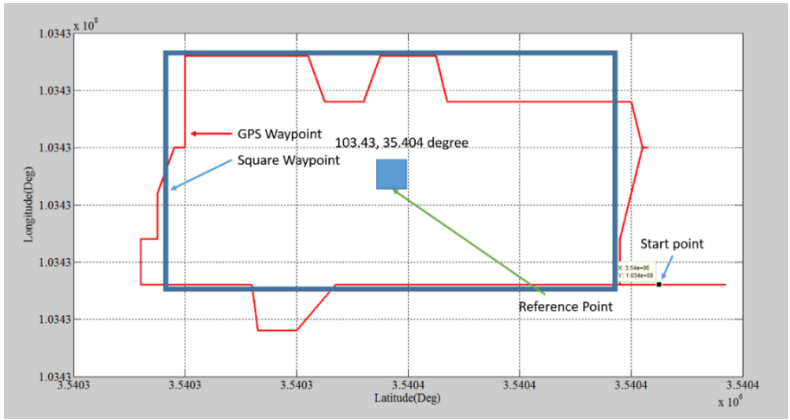

Fig.32. Generated localization of square movement of MHeLFAGV

As for the first validation, the rectilinear motion is designed as MHeLFAGV trajectory input from joystick whereby it is a combination of side right, forward, backward, and side right vector movements as shown in Figure 32. The experiment is further with the diagonal motion on MHeLFAGV whereby this motion is a combination of side right, forward, rotate, and side left vector movement as depicted in Figure 33. The MHeLFAGV is also moved according to the reference point place center of square waypoint as shown in Figure 34.

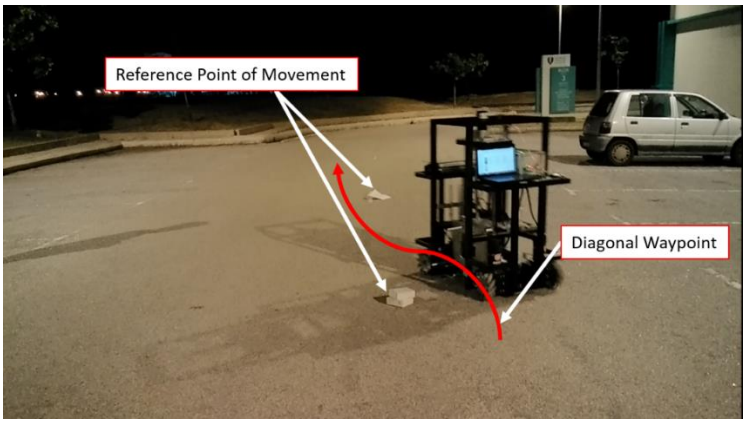

Fig. 33. Snapshot of diagonal motion experiment on the MHeLFAGV system

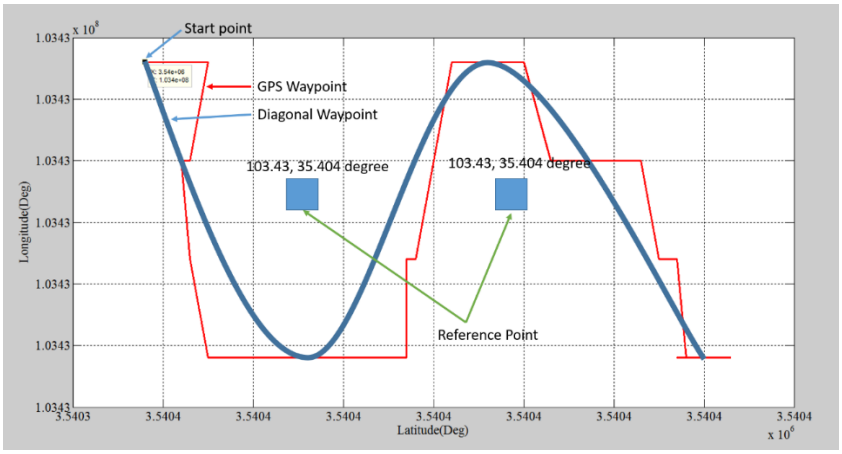

Fig. 34. Generated localization of diagonal movement of MHeLFAGV

The series of zigzagging motion then is done in which combination of diagonal right, diagonal left, rotate, and vice versa vector movement as shown in Figure 35 and 36. A similar methodology is repeated for rounding motion as shown in Figure 37 and 38. This motion is the combination of the basic motion of mecanum such as side right, forward, rotate, and side left vector movement. Overall results show generated localization having error slightly to follow the targeted trajectory. This is due to friction and uneven surface of the terrain during testing sessions.

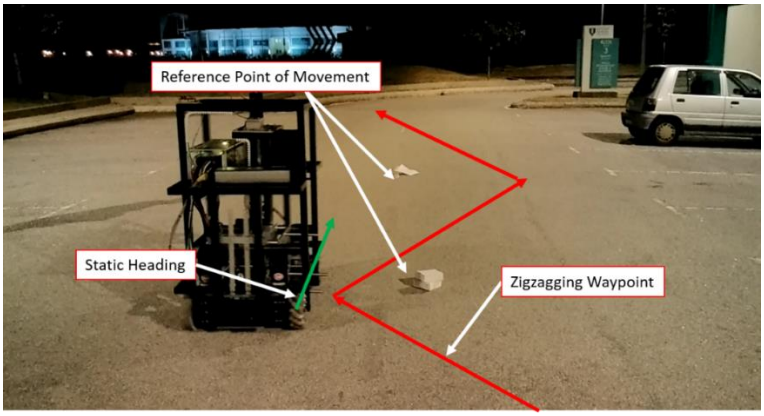

Fig. 35. Snapshot of zigzagging motion experiment on the MHeLFAGV system

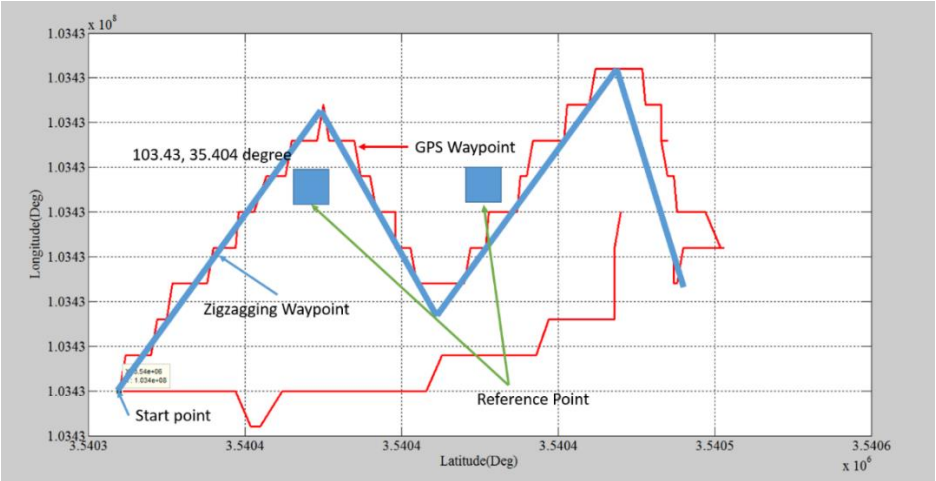

Fig. 36. Generated localization of zigzagging movement of MHeLFAGV

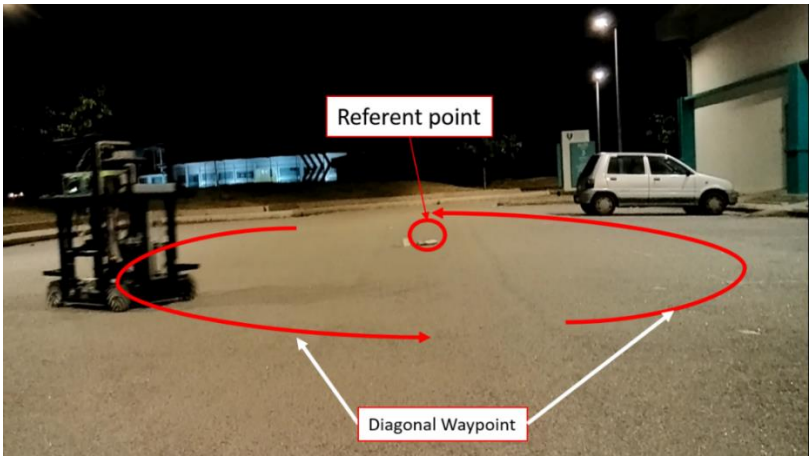

Fig. 37. Snapshot of rounding motion experiment on MHeLFAGV system

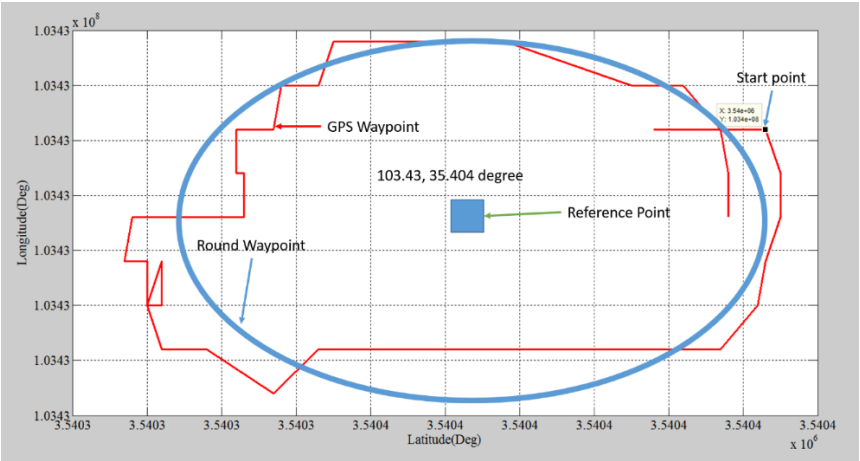

Fig. 38. Generated localization of rounding movement of MHeLFAGV

5.4. Forklifting Precision Experiment and Analysis

In order to verify the proposed Antiwindup with TSK-FLC as discussed in Section IV, several experiments were conducted to observe the performance and effect on the axis motion precision of MHeLFAGV Forkloader. The emphasis of the experiments is on *Y*-axis motion performance; a similar method was applied to the *X*-axis using different parameter tuning. A repeating sequence stair signal is used to generate the reference or desired position, with gap distance ranging from 25 cm to 50 cm from the ultrasonic sensor. The experiment was done in two sessions with the same desired input: *Y*-axis movement with TSK-FLC, and *Y*-axis with Antiwindup-TSK-FLC (A-TSK-FLC). Some fine tuning was done on each tuning parameter, such as K_p and K_D for TSK-FLC and, K_i and K_T, for A-TSK-FLC. As shown in Figure 50, the experiment is done and analyzed in two cases: *Y*-axis movement from 25 cm point to 50 cm and vice versa.

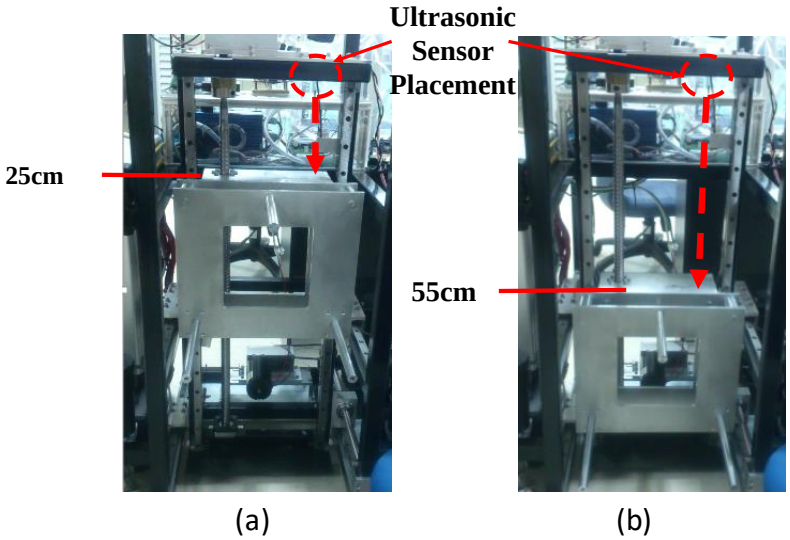

Fig. 38. Experimental setting for forkloader *Y*-Axis position from MHeLFAGV top frame: (a) at 25 cm, (b) at 55 cm

For the case of movement from 25 cm to 50 cm, A-TSK-FLC settling time is able to response 3.7s faster than that of the *Y*-axis motion with TSK-FLC, as shown in Figure 51. Also, the overshoot that occurred in the case of TSK-FLC causes instability in its operation, which amounts to about 80% from

the steady-state position. Moreover, the oscillation that produces swinging on Forkloader unit its entirely decay the settling time for this running, which takes about 6sec from the first move. It is different to the A-TSK-FLC running whereby almost no overshoot occurred when the Forkloader unit achieved 50 cm point from distance sensor. On the other hand, A-TSK-FLC running able to achieve settling time is 3.7s faster than TSK-FLC. The almost same situation occurred in the case of positioning from 25 cm to 50 cm point. TSK-FLC and A-TSK-FLC operate in the same manner regarding time response; however, as shown in Figure 51, an overshoot of about -50% from the desired position occurred when operating in TSK-FLC, may risk the full item. Also, due to the overshoot, oscillation also occurred in this point of positioning for the case of *Y*-axis movement with TSK-FLC, in which the settling time is delayed by about 2.1 s compared to that of the A-TSK-FLC.

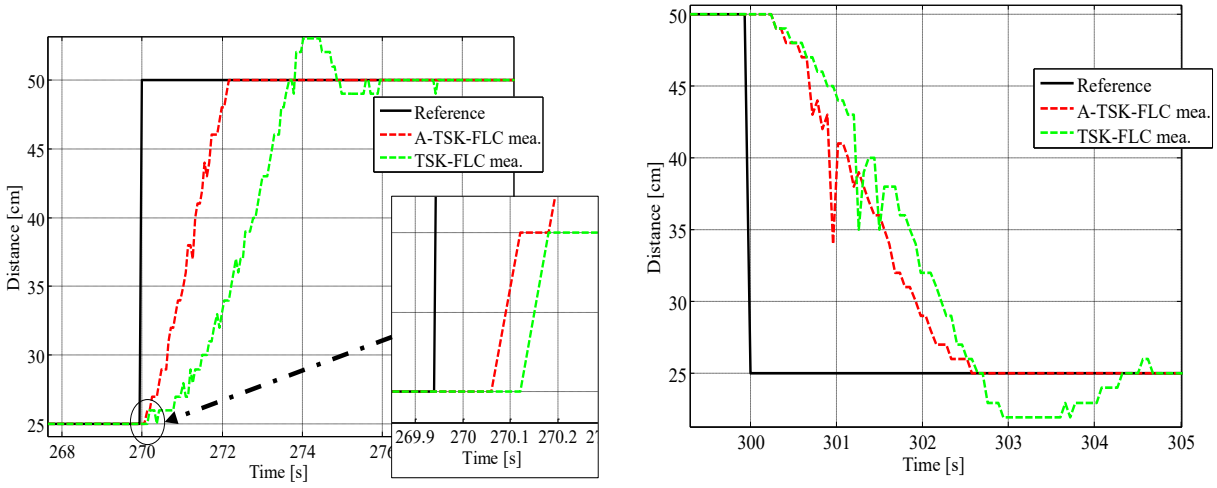

Fig. 39. A-TSK-FLC (red) versus TSK-FLC (green) Y-axis experiment sample: (a) for motion from 25 cm to 50 cm positioning, (b) for motion from 50 cm to 25 cm positioning

Locking mechanism load performance analysis has been conducted to test for the capability of locking mechanism's mechanical power transmission performance. The locking mechanism is tested using a different weight of the load. The time taken for the locking mechanism to rotate to lock position and back again to unlock position is recorded for each load used. The analysis also has been carried out to measure the cycle of locking mechanism that can be operated until the battery voltage has dropped for about 10% from its initial voltage. The more massive the load used in operation, the longer the time taken. The increased pattern of the time taken for the operation is shown in Figure 52. This result shows that the locking mechanism has successfully achieved the targeted operation duration which is below than 3 seconds. The same goes for average starting and steady current which have been increasing as the spool weight increased as shown in Figure 53 and Figure 54 respectively. This is because the power consumption also increased as the load used increased.

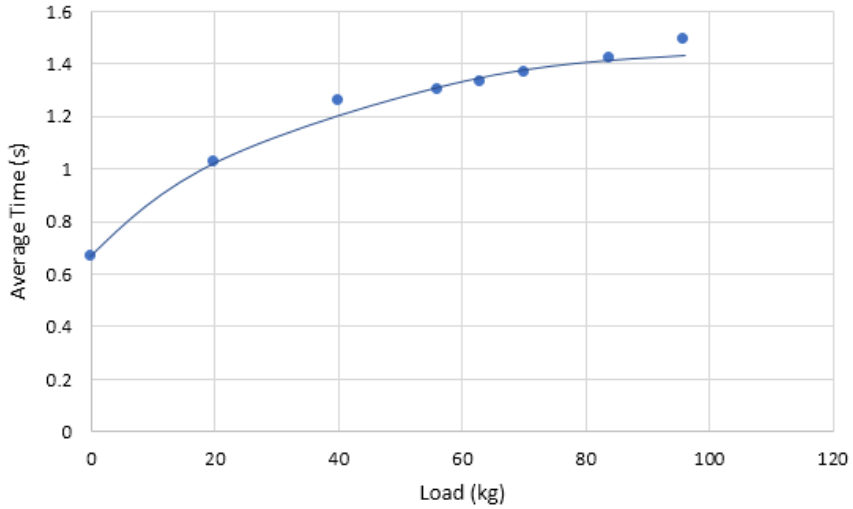

Fig. 40. Load versus locking time

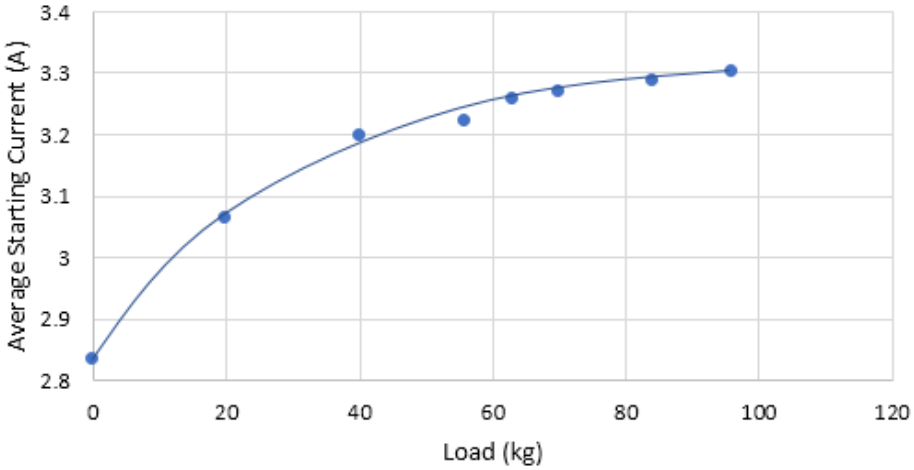

Fig. 41. Load versus average starting current

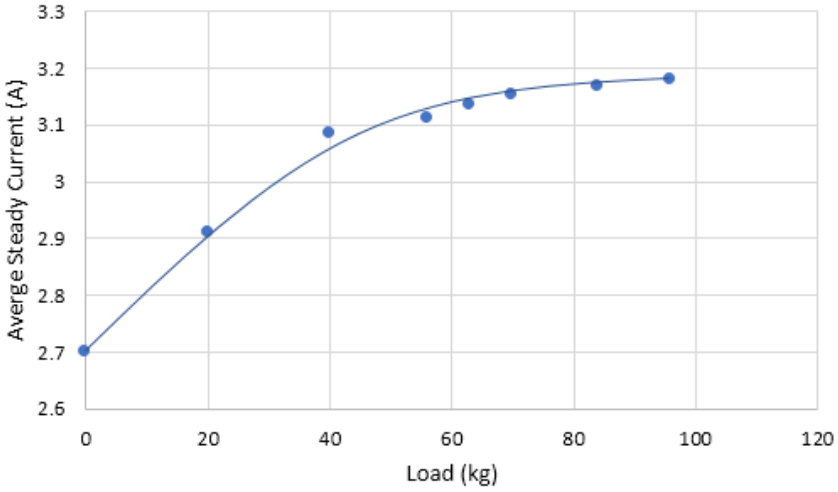

Fig. 42. Load versus average steady current

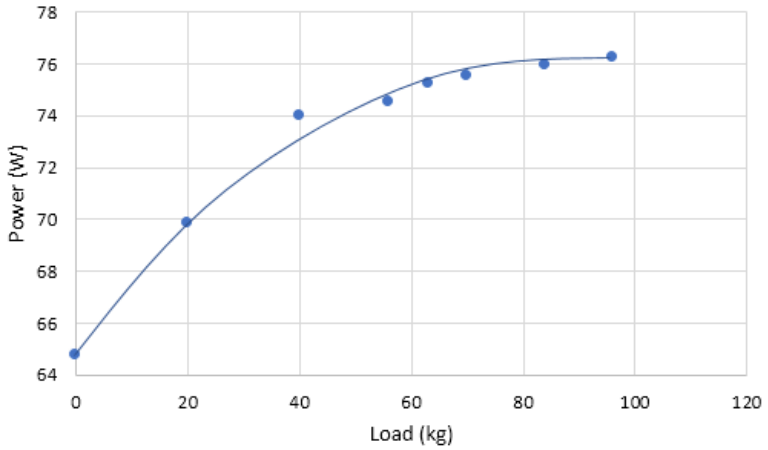

Fig. 43. Load versus power consumed by the servo

A similar pattern is shown in load versus power consumed by servo motor as shown in Figure 55. Concerning the battery performance from the record for every 25 cycles from the fully charged voltage of the battery which is 27.90 V until 26.51 V, the voltage was dropped continuously at about 0.1 V to 0.2 V after every 25 cycles of mechanical process as shown in Figure 56. The sudden-dropped voltage does not appear according to this performance, and this has validated that the proposed locking system is reliable for the MHeLFAGV system.

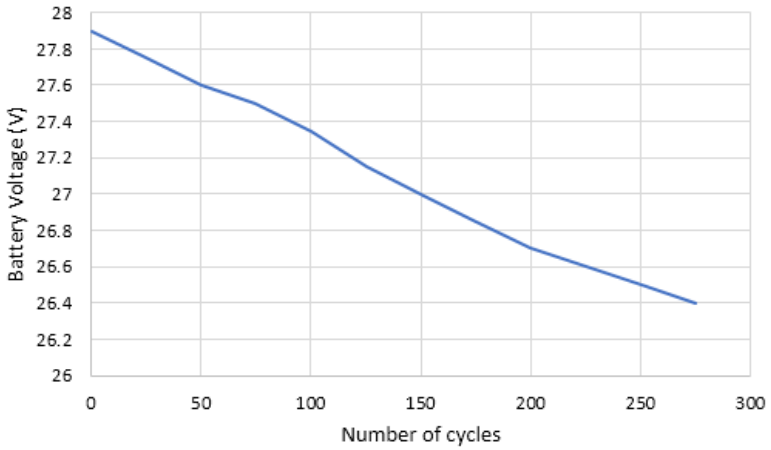

Fig. 44. A number of cycles versus battery usage in volt

6. Conclusion

The development of mini AGV with forklift named MHeLFAGV has been discussed thoroughly and the performance of its functions have been presented. With the verification of MHeLFAGV structure shows that this system able to handle heavy payload as targeted which is about 20-200kg. On the other hand, with RF as wireless communication for remotely control and mecanum wheel as its tire, the experimental results show that this MHeLFAGV able operate in an omnidirectional mode that allows unchanged position on its body. This is very crucial especially when MHeLFAGV will take a turn at the cornering path. On the other hand, designed fork-loader unit programmed with the advanced control system, antiwindup PD-FLC, that performed high precision on both axes. On the other hand, the proposed CHT seems improving the image processing for the autonomous picking and alignment for MHeLFAGV when handling a copper spool picking at the warehouse. The overall validation shows

that this first phase of prototype ready to be deployed with major on remotely control mode. The next step in this research is to proceed with the next phase of development that emphasized more on gaining the autonomous function in MHeLFAGV as its name implied. The most part that will be emphasized is on precision in picking and placing copper spool, collision avoidance and autonomous moving on track.

7. Acknowledgment

This research and development are supported by the Universiti Malaysia Pahang (UMP) Research Grant (RDU180332) through Advanced Engineering Automotive Centre (AEC), and major technically supported by Vacuumshmelze (M) Sdn. Bhd.

References

[1] Lee, Young-Jin, Jin-Ho Suh, Jin-Woo Lee, and Kwon-Soon Lee. "AGV steering controller using NN identifier and cell mediated immune algorithm." In *American Control Conference, 2004. Proceedings of the 2004*, vol. 6, pp. 5778-5783. IEEE, 2004.

[2] Ismail, Ir Idris, and Mohd Fariz Nordin. "Reactive navigation of autonomous guided vehicle using fuzzy logic." In *Research and Development, 2002. SCOReD 2002. Student Conference on*, pp. 153-156. IEEE, 2002.

[3] Lee, Young Jin, Jin Ho Suh, Jin Woo Lee, and Kwon Soon Lee. "Adaptive PID control of an AGV system using humoral immune algorithm and neural network identifier technique." In *Control Applications, 2004. Proceedings of the 2004 IEEE International Conference on*, vol. 2, pp. 1576-1581. IEEE, 2004.

[4] Lee, Young Jin, Sang Ki Kim, and Kwon Soon Lee. "Auto steering control of unmanned container transport (UCT) with vision system and mediated immune algorithm controller." In *Industrial Electronics Society, 2004. IECON 2004. 30th Annual Conference of IEEE*, vol. 3, pp. 2987-2991. IEEE, 2004.

[5] Borowiecki, Tomasz, and Zbigmew Banaszak. "A constraint programming approach for AGVs flow control." In *Robot Motion and Control, 1999. RoMoCo'99. Proceedings of the First Workshop on*, pp. 153-158. IEEE, 1999.

[6] Chiba, Ryosuke, Jun Ota, and Tamio Arai. "Design of robust flow-path network for AGV systems using competitive co-evolution with packaging." In *Intelligent Robots and Systems, 2005.(IROS 2005). 2005 IEEE/RSJ International Conference on*, pp. 3137-3142. IEEE, 2005.

[7] Kiinemund, Frank, Daniel Heß, Matthias Wißing, and Christof Röhrig. "Online kinodynamic motion planning for omnidirectional automatic guided vehicles." In *Control Automation Robotics & Vision (ICARCV), 2014 13th International Conference on*, pp. 1778-1783. IEEE, 2014.

[8] Azenha, Abílio, and Adriano Carvalho. "A neural network approach for AGV localization using trilateration." In *Industrial Electronics, 2009. IECON'09. 35th Annual Conference of IEEE*, pp. 2699-2702. IEEE, 2009.

[9] Perez-Ramirez, Javier, Deva K. Borah, and David G. Voelz. "Optimal 3-D landmark placement for vehicle localization using heterogeneous sensors." *IEEE Transactions on Vehicular Technology* 62, no. 7 (2013): 2987-2999.

[10] Zhang, Jiantao, Chunbo Zhu, and C. C. Chan. "A wireless power charging method for automated guided vehicle." In *Electric Vehicle Conference (IEVC), 2014 IEEE International*, pp. 1-5. IEEE, 2014. \

[11] Chen, Hong-Ming, Yi-Ping Shyu, Chun-Sheng Shen, and Hong-Jia Yang. "The picked and placed control of the objects for a pneumatic XY servo platform by integrating image processing techniques and a fuzzy sliding mode controller design." In *Fuzzy Systems (FUZZ), 2011 IEEE International Conference on*, pp. 1127-1133. IEEE, 2011.

[12] Kotthauser, Tobias, and Georg F. Mauer. "Vision-based autonomous robot control for pick and place operations." In *Advanced Intelligent Mechatronics, 2009. AIM 2009. IEEE/ASME International Conference on*, pp. 1851-1855. IEEE, 2009.

[13] Irawan, A, and A. Razali, R. "Forklift for Confine Area." In *Malaysia Intellectual Properperties Organization (MyIPO)*, edited by Universiti Malaysia Pahang. Malaysia, 2017.

[14] Vlantis, Panagiotis, Charalampos P. Bechlioulis, George Karras, George Fourlas, and Kostas J. Kyriakopoulos. "Fault tolerant control for omni-directional mobile platforms with 4 mecanum wheels." In *Robotics and Automation (ICRA), 2016 IEEE International Conference on*, pp. 2395-2400. IEEE, 2016.

[15] Hao, Yongxin, Xu Dong, Jianxiang Li, Shiyou Mu, and Xingzhao Wang. "Mecanum wheeled motion system with three wheels." In *Applied Robotics for the Power Industry (CARPI), 2016 4th International Conference on*, pp. 1-4. IEEE, 2016.

[16] Astrom, K. J., and Björn Wittenmark. "Adaptive control. mineola." (2008).

[17] Irawan, A, and A. R. Razali. "Forklift for Confine Area." In *Intellectual Property Corporation of Malaysia (MyIPO)*, edited by Universiti Malaysia Pahang, 2017.

[18] Irawan, Addie, Kenzo Nonami, and Mohd Razali Daud. "Optimal impedance control with tsk-type flc for hard shaking reduction on hydraulically driven hexapod robot." In *Autonomous Control Systems and Vehicles*, pp. 223-236. Springer, Tokyo, 2013.

[19] Takagi, Tomohiro, and Michio Sugeno. "Fuzzy identification of systems and its applications to modeling and control." *IEEE transactions on systems, man, and cybernetics* 1 (1985): 116-132.

[20] Lezaini, Wan, Wan Mohd Nafis, Addie Irawan, and Sheikh Norhasmadi Sheikh Ali. "Forkloader Position Control for A Mini Heavy Loaded Vehicle using Fuzzy Logic-Antiwindup Control." *Telkomnika* 15, no. 2 (2017).

[21] Markaroglu, Hayk, Mujde Guzelkaya, Ibrahim Eksin, and Engin Yesil. "Tracking time adjustment in back calculation anti-windup scheme." In *Proceedings 20th European Conference on Modelling and Simulation*. 2006.

[22] Strang, Gilbert, and George J. Fix. *An analysis of the finite element method*. Vol. 212. Englewood Cliffs, NJ: Prentice-hall, 1973.